

Substrate temperature and water vapour effects on structural and mechanical properties of TiO_xN_y coatings

J. M. Chappé · J. Gavaille · N. Martin ·
J. Lintymer · J. Takadoum

Received: 30 August 2005 / Accepted: 31 October 2005 / Published online: 20 June 2006
© Springer Science+Business Media, LLC 2006

Abstract Dc reactive sputtering was successfully implemented to deposit titanium oxynitride thin films using a titanium metallic target, argon, nitrogen and water vapour as reactive gases. The nitrogen partial pressure was kept constant during every deposition whereas that of the water vapour was systematically changed from 0 to 0.1 Pa. The study aims at comparing the structural and mechanical properties of the coatings deposited at room temperature (293 K) and at 673 K. Surface morphology of the film was examined by atomic force microscopy and showed different aspects according to the growth temperature. Topography mainly depends on the amount of water vapour introduced during the deposition process. Some significant changes of the crystallographic structure, due to the high substrate temperature were correlated with the evolution of the surface aspect and roughness parameters. Determination of the phase occurrence by X-ray diffraction was also carried out and appeared to be a significant parameter in understanding the evolution of mechanical properties like nanohardness (H_n) and Young's modulus (E). H_n and E values obtained by nanoindentation ranged from 16.5 to 7 GPa and from 240 to 100 GPa, respectively. For both temperatures, mechanical properties of titanium oxynitride thin films were notably reduced as a function of the water vapour supply, especially for partial pressures higher than

4×10^{-2} Pa. These mechanical behaviours were correlated and discussed with the phase occurrence and the amorphous structure of titanium oxynitride thin films.

Introduction

For several years, metallic oxynitride compounds have gained scientific interest because of their versatile properties [1–3]. They have been prepared by various chemical and physical deposition techniques. Among these types of films, titanium oxynitride thin films have been one of the most intensively studied systems [4–7]. Recent works on TiON coatings with a tuneable N/O ratio showed that they exhibit a complex structure and revealed intermediate behaviours between metallic TiN and insulating TiO_2 compounds [8–10]. Indeed titanium oxynitrides benefit from properties of metallic oxides (colours, optical properties like refractive index, chemical stability) and nitrides (hardness, wear resistance). Physical vapour deposition and especially reactive magnetron sputtering is an attractive way to deposit these films. A titanium target sputtered in a mixed working gas ($\text{O}_2 + \text{N}_2$) [11] or the reactive gas pulsing technique [4, 12] can be used to modify the metalloid concentrations in the films. An alternative to O_2 gas as an oxygen source is water vapour. To the best of our knowledge, such a reactive gas has almost never been used for reactive magnetron sputtering of oxides [13–15] and rarely for the deposition of titanium oxynitrides [16]. Few works focused on the electrical properties of transparent conductive oxides (TCO) showed a small decrease of the conductivity when water vapour is added to the sputtering atmosphere [17, 18]. Recently, the conductivity of

J. M. Chappé · J. Gavaille · N. Martin (✉) · J. Lintymer ·
J. Takadoum

Laboratoire de Microanalyse des Surfaces (LMS), Ecole
Nationale Supérieure de Mécanique et des Microtechniques
(ENSMM), 26, Chemin de l'épitahe, 25030 Besançon Cedex,
France
e-mail: nicolas.martin@ens2m.fr

amorphous indium tin oxide (ITO) coatings was shown to significantly increase when water vapour was used as reactive gas [19].

In this work, we report on the influence of the substrate temperature on structural and mechanical properties of titanium oxynitride thin films deposited by dc reactive magnetron sputtering. Water vapour is chosen as the reactive gas to provide oxygen into the sputtering process. Substrate temperature and water vapour partial pressure are the key parameters in this study. Mechanical properties and surface topography of as-deposited coatings are then related to the crystallographic structure of the films deposited at 293 K (set A) and 673 K (set B).

Experimental

The deposition of titanium oxynitride thin films was performed in a home-made high vacuum reactor with a 40 L volume. Glass and (100) silicon substrates were introduced through a 1 L load-lock system. An ultimate pressure of 10^{-5} Pa was obtained with a turbomolecular pump backed with a mechanical pump. The reactor was equipped with a circular planar and water cooled magnetron sputtering source. It allows us to keep at a constant temperature $T_A = 293$ K (set A) or $T_B = 673$ K (set B) the grounded substrates, which are made from glass micro slides and (100) silicon wafers. A metallic titanium target (purity 99.6% and 50 mm diameter) was dc sputtered with a constant current density $J_{Ti} = 51$ A m⁻². It was located at a distance of 65 mm from the substrates. Before each run, substrates were ultrasonically cleaned with acetone and alcohol, and the titanium target was pre-sputtered in a pure argon atmosphere for 5 min in order to remove the contamination layer at the surface of the target. Afterwards, nitrogen and water vapour reactive gases were introduced and the deposition stage was started after few minutes of stabilization. Argon and nitrogen partial pressures were maintained at 0.4 and 0.1 Pa, respectively, using mass flow controllers and a constant pumping speed S of 24.7 L s⁻¹. The water vapour partial pressure was systematically changed from 0 to 0.1 Pa using a leak valve connected to a de-ionized water flask. Its value was given by subtracting nitrogen and argon partial pressures from the total pressure (plasma on) [16]. The deposition time was adjusted in order to obtain a thickness close to 400 nm (measured by a Dektak IIA mechanical profilometer). Substrates were left at room temperature (293 K) for set A and kept at 673 K for set B by a resistive heater, which maintained the temperature within ± 15 K.

The crystallographic structure was investigated by X-ray diffraction (XRD) using monochromatic Cu K_α radiation at a grazing incidence angle $\theta = 1^\circ$. The chemical

composition of the films deposited on silicon wafer (100) was determined by Rutherford backscattering spectroscopy and nuclear reaction analysis [16]. Surface morphology and roughness were investigated by atomic force microscopy (AFM) in contact mode. Three scans of 4 μm² were carried out for each film in order to obtain a representative surface aspect. Hardness and reduced Young's modulus of the films were determined by nanoindentation with a sinusoidal mode using a Berkovich nanoindenter.

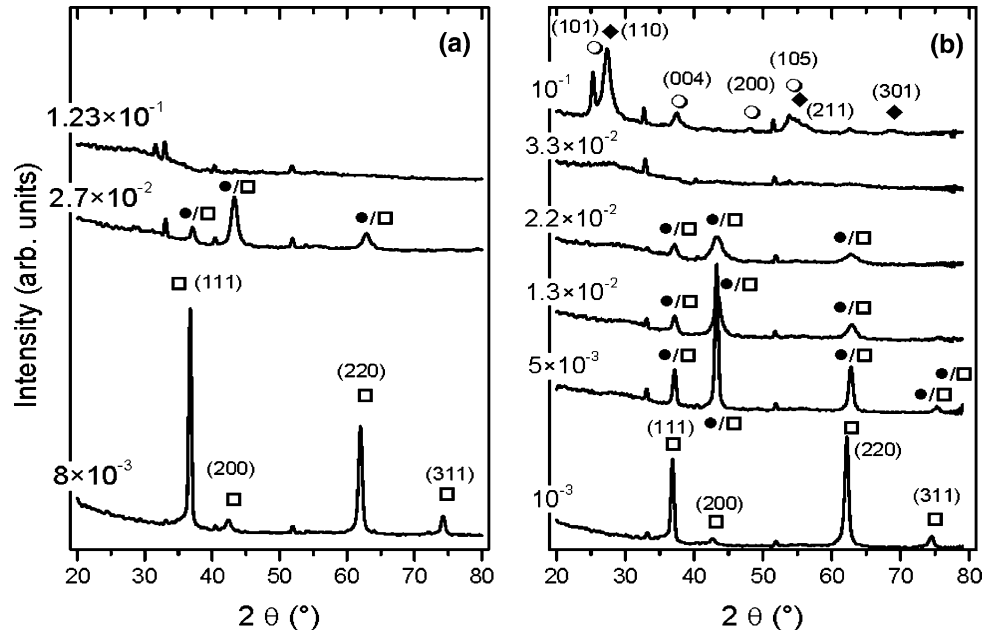
Results and discussion

Crystallographic structure

The phase occurrence of both series (A and B) deposited on (100) Si substrates was investigated by XRD (Fig. 1). For set A, without water vapour introduction and up to $P_{H_2O} = 8.0 \times 10^{-3}$ Pa, peaks corresponding to the f.c.c. phase appear with a preferential orientation along the [111] direction. This kind of nano-structured compound, with a crystallite size about 20 nm (revealed by the Scherrer's method), tends to disappear when the water vapour pressure exceeds 8.0×10^{-3} Pa. Orange-brownish coatings become dark green titanium oxynitrides. They still exhibit diffracted signals corresponding to a structure based on an f.c.c. lattice. Since TiO and TiN compounds both adopt the same crystallographic structure (f.c.c.) with neighbour lattice parameter ($a_{TiN} = 0.424$ nm and $a_{TiO} = 0.419$ nm), XRD technique is not a suitable method to distinguish between these two structures, especially for poorly crystallized coatings. The films may be composed of two phases: a weakly crystallized f.c.c. phase and an amorphous one. A further increase of the water vapour partial pressure leads to an amorphization of the films. As a result, when the water vapour pressure is higher than 1.2×10^{-1} Pa, titanium oxynitride coatings are completely amorphous (Fig. 1-a).

For set B, the preferential orientation along the [111] direction previously observed for set A is not so significant up to $P_{H_2O} = 1.0 \times 10^{-3}$ Pa since the [220] signal also shows a strong intensity (Fig. 1-b). The substrate temperature kept at 673 K gives rise to the surface diffusion of sputtered particles impinging on the growing film. It favours more equiaxed grains rather than a growth along some preferential directions. For water vapour partial pressures higher than 5.0×10^{-3} Pa, diffracted signals corresponding to a structure based on an f.c.c. lattice become less intense and broader. The [220] growth direction is preferred until P_{H_2O} reaches 2.2×10^{-2} Pa and the crystal size is largely reduced (few nanometers). For these values of water pressure, the long range order disappears and an amorphous structure is obtained at

Fig. 1 X-ray diffraction patterns of titanium oxynitride thin films deposited on (100) silicon wafers at (a) 293 K (set A) and (b) 673 K (set B). □ = TiN; ● = TiO; ◆ = Rutile; ○ = Anatase

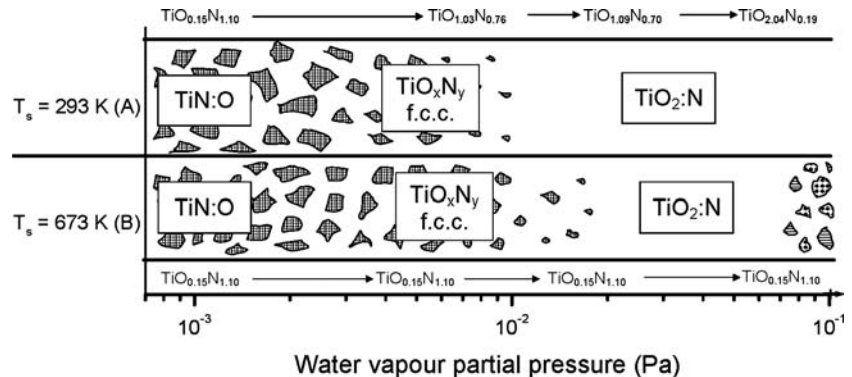


$P_{H_2O} = 3.3 \times 10^{-2}$ Pa. A further introduction of water clearly produces the coexistence of anatase and rutile TiO_2 phases (Fig. 1-b) whereas amorphous compounds are deposited at room temperature for a similar range of water vapour partial pressures (Fig. 1-a). The substrate temperature (set B) and the amount of water vapour introduced into the process are high enough to produce the most stable phases of TiO_2 compound.

The distribution of structures in zones represented in Fig. 2 is peculiar to the parameters described by the authors above. It can not be taken as an overall structural model. Such distribution allows us to compare phase occurrence with mechanical properties (see section 3.3). Elemental concentration is also indicated in this diagram. It is worth of noting the reverse evolution of oxygen and nitrogen contents. Thus, substrate temperature and water vapour partial pressure are the two key parameters, which influence the crystallographic structure of titanium oxynitride thin films as well as their chemical composition. It

is worth to note that the f.c.c. phase is systematically obtained for a wide range of water vapour pressures. Such a range is shifted to lower values as temperature increases (more than 3.0×10^{-3} Pa for set A against 2.2×10^{-2} Pa for set B). This is due to the highest reactivity of titanium towards oxygen compared to nitrogen, which rises with temperature. Then the occurrence of the amorphous structure is also moved to lower water vapour partial pressures in a narrow window ($2.2 \times 10^{-2} < P_{H_2O} \leq 3.3 \times 10^{-2}$ Pa). Above $P_{H_2O} = 3.3 \times 10^{-2}$ Pa, crystallized TiO_2 compound is favoured since the diffraction patterns reveal several peaks corresponding to anatase and rutile phase mixture. It is in agreement with previous results obtained by Lobl et al. [20]. The authors developed an experimental diagram showing qualitatively the conditions for the occurrence of amorphous, anatase, or rutile titanium dioxide thin films. Substrate temperature and energy of the particles impinging on the substrate are the relevant parameters. They claimed that a substrate temperature

Fig. 2 Phase occurrence in titanium oxynitride films versus water vapour partial pressure at room temperature (set A) and 673 K (set B). The chemical composition of the films determined by Rutherford backscattering spectroscopy and nuclear reaction analysis is also indicated for both sets. ■ f.c.c. phase □ amorphous ▤ Rutile ▨ Anatase



included between 473 K and 673 K is required to get an anatase + rutile phase mixture.

Surface topographic analysis

The surface topographic analysis performed by AFM shows different aspects of the films deposited on glass substrates (Fig. 3). Without water vapour injection and for both temperatures, the surface morphology of the films exhibits a sharp nodular shape (close to 100 nm wide peaks) whereas an injection of water vapour leads to larger and more distant nodules. Indeed at $P_{\text{H}_2\text{O}} = 0$ Pa, the surface is homogeneous and made of regularly spaced and similar peaks of 70 nm maximum height for both sets (Fig. 3a and c). Mean roughness values (Table 1) are $R_a = 6.4 \pm 0.5$ nm for room temperature deposited coatings (set A) and $R_a = 7.5 \pm 0.4$ nm for coatings deposited at 673 K (set B). For room deposition temperature (set A), water vapour induces a heterogeneous surface even for low water vapour pressures (Fig. 3b). The surface aspect is composed of larger and more spaced peaks. R_a decreases continuously when $P_{\text{H}_2\text{O}}$ rises, down to a minimum value of 2.9 ± 1.1 nm. Such a lowest roughness corresponds to the formation of an amorphous titanium oxynitride compound. Coatings deposited at 293 K and with water vapour pressures higher than $P_{\text{H}_2\text{O}} = 1.7 \times 10^{-2}$ Pa also exhibit a smooth aspect. As a result, the flattening phenomenon of the titanium oxynitride surface can also be correlated to the phase occurrence diagram suggested previously (Fig. 2).

At 673 K (set B) and for $P_{\text{H}_2\text{O}} = 4.0 \times 10^{-3}$ Pa, the surface is smoother with cauliflower-shaped domes (maximal height of 112 nm in Fig. 3d). Here again, the mean roughness still reveals the smallest value for titanium oxynitride thin films adopting an amorphous structure. This correlation has already been noticed by Hones et al. [21] on sputter deposited chromium oxide thin films. Although, measurements of the films' density by Rutherford back-scattering spectroscopy and nuclear reaction analysis did not reveal any correlation between an amorphous structure and a high density that could explain a low roughness [16].

Mechanical properties

Nanoindentation was performed in a dynamic mode with continuous stiffness measurements. A maximum load of 2 mN was applied. Unloading stiffness gave the reduced Young's modulus and nanohardness of the films with the Oliver and Pharr's method, knowing the real contact area [22]. Films are around 400 nm thick and indentations were made at 10% depth in order to minimize the influence of the substrate on the final results [23]. Fig. 4 shows the evolution of nanohardness (H_n) of titanium oxynitride thin films as a function of the water vapour partial pressure. Up to $P_{\text{H}_2\text{O}} = 2.8 \times 10^{-2}$ Pa and for coatings deposited at 673 K (set B), nanohardness is quite stable and slightly decreases from 16.6 to 15 GPa. For highest water vapour pressures, H_n abruptly drops and finally remains nearly constant close to 11 GPa in spite of a large increase of the

Fig. 3 AFM images of titanium oxynitride films with (a) $P_{\text{H}_2\text{O}} = 0$ Pa, $T_s = 293$ K; (b) $P_{\text{H}_2\text{O}} = 1.7 \times 10^{-2}$ Pa, $T_s = 293$ K; (c) $P_{\text{H}_2\text{O}} = 0$ Pa, $T_s = 673$ K and (d) $P_{\text{H}_2\text{O}} = 4 \times 10^{-2}$ Pa, $T_s = 673$ K

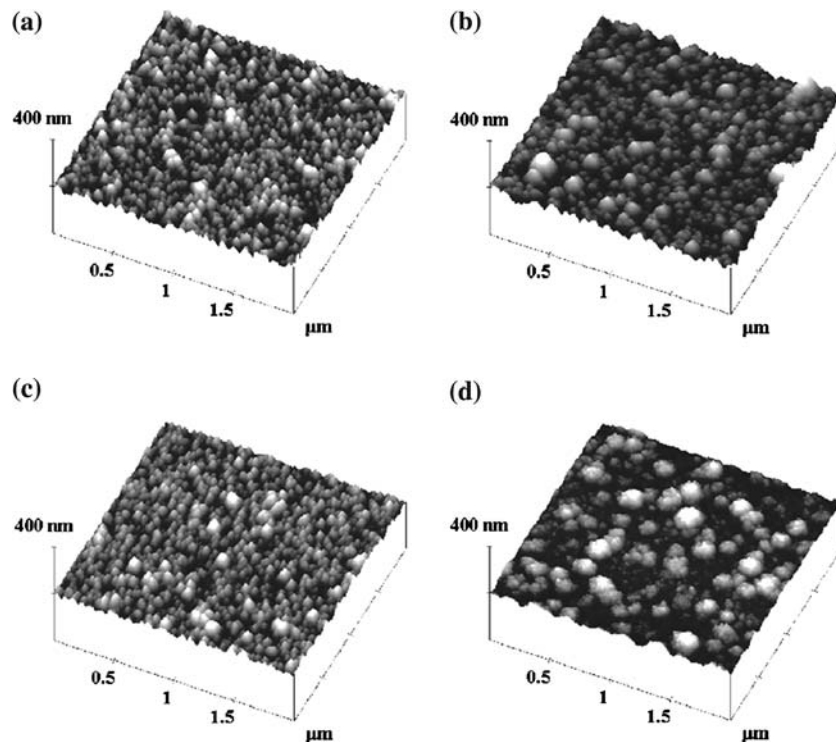
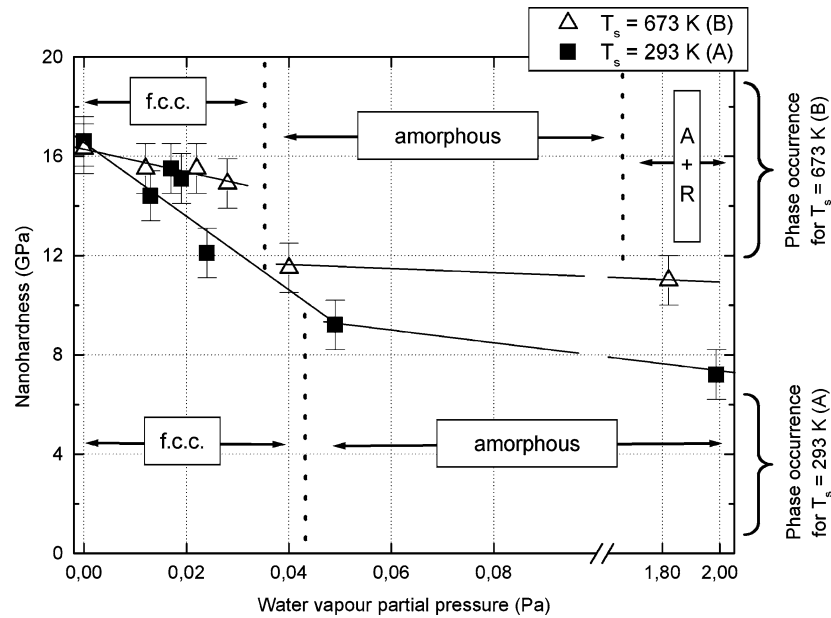


Table 1 Mean roughness as a function of the substrate temperature and water vapour partial pressure

$T = 293 \text{ K (set A)}$		$T = 673 \text{ K (set B)}$	
$P_{\text{H}_2\text{O}}$ (Pa)	R_a (nm)	$P_{\text{H}_2\text{O}}$ (Pa)	R_a (nm)
0	6.4 ± 0.5	0	7.5 ± 0.4
1.5×10^{-2}	5.8 ± 1.0	1.2×10^{-2}	5.6 ± 0.7
1.7×10^{-2}	6.0 ± 0.3	2.2×10^{-2}	7.7 ± 4.6
3.4×10^{-2}	5.0 ± 1.1	2.8×10^{-2}	2.1 ± 0.2
4.9×10^{-2}	2.9 ± 1.1	4.0×10^{-2}	9.4 ± 0.5
		1.8	5.4 ± 2.6

Fig. 4 Influence of the water vapour partial pressure on nanohardness of titanium oxynitride films prepared at 293 K (set A) and 673 K (set B); A + R = Anatase + Rutile



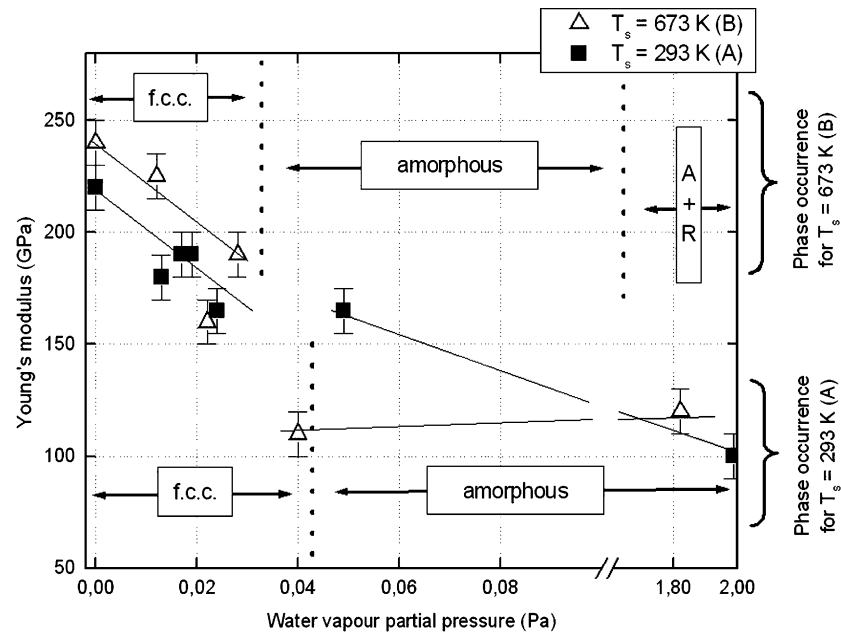
water vapour partial pressure ($P_{\text{H}_2\text{O}} = 1.8 \text{ Pa}$). Some similar behaviours are measured for films deposited at room temperature (set A) with a more significant reduction of H_n down to 9.2 GPa when $P_{\text{H}_2\text{O}}$ reaches $4.9 \times 10^{-2} \text{ Pa}$. Afterwards, nanohardness is less influenced by the water vapour introduction. Besides, this limit is also described by Makino et al. [24] as the beginning of the drop of the film hardness. They measured a maximal H_n for an oxygen content of 30%, which nearly corresponds to the point located at $P_{\text{H}_2\text{O}} = 2.8 \times 10^{-2} \text{ Pa}$ [16].

It is worth of comparing nanohardness of the films to the phase occurrence diagram suggested previously (Fig. 2). Thus, the highest hardness is measured when titanium oxynitride compounds adopt the f.c.c. phase. A decrease of the f.c.c. crystal size well correlates with the reduced nanohardness and in the same way, amorphization of the films corresponds to the stable H_n values. Here again, coatings deposited at room temperature (set A) exhibit the wide range of hardness and f.c.c. occurrences ($P_{\text{H}_2\text{O}}$ higher than $4.9 \times 10^{-2} \text{ Pa}$). The highest hardness values always achieved at 673 K (set B) can be attributed to a more compact structure of the films, which is favoured at high

temperature. As expected, a low hardness (11 GPa) is also obtained for coatings composed of anatase + rutile phase mixture (set B) since these coatings can be assumed as TiO_2 compound with nitrogen as doping.

Similarly, reduced Young’s modulus versus water vapour partial pressure reveals a comparable evolution to nanohardness (Fig. 5). For both sets, an increasing water injection in the sputtering process leads to a significant decrease of reduced Young’s modulus from 220–240 down to 100–110 GPa. Modulus is gradually reduced for titanium oxynitride thin films deposited at room temperature (set A). On the other hand, modulus of coatings prepared at 673 K (set B) exhibits an abrupt drop for $P_{\text{H}_2\text{O}} = 4.0 \times 10^{-2} \text{ Pa}$. As previously noticed for hardness, it relates to the vanishing of f.c.c. phase and amorphization phenomenon of the films. The evolution of reduced Young’s modulus with water vapour partial pressure can also be correlated with the decrease of the crystal size (Fig. 1), which implies a high density of grain boundaries [25]. These grain boundaries hinder the dislocation migration in the f.c.c. phase and hence limit the plastic deformation induced by the indentation. The grain size becomes small enough to

Fig. 5 Influence of the water vapour partial pressure on reduced Young's modulus of titanium oxynitride films deposited at 293 K (set A) and 673 K (set B); A + R = Anatase + Rutile



permit the crack propagation around the crystallites and, therefore, the blocking effect of grain boundaries is no longer effective [26].

Conclusion

Titanium oxynitride thin films were successfully deposited by dc reactive magnetron sputtering with nitrogen and water vapour as reactive gases. The influence of the substrate temperature (room temperature and 673 K) on the phase occurrence, surface morphology and mechanical properties of the films was investigated. It was shown that for low water vapour partial pressures, titanium oxynitride systematically adopted an f.c.c. phase for any deposition temperature. This f.c.c. vanished with a further supply of water vapour into the sputtering process and led to an amorphization of the films prepared at room temperature or an anatase + rutile phase mixture at 673 K. Surface morphology analyses revealed a nodular aspect of the surface topography. This latter depended on the amount of water vapour partial pressure and a flattening of the surface was correlated with an amorphization of the films. Mechanical properties determined by nanoindentation showed that the water vapour partial pressure remained the predominant parameter in the evolution of the nanohardness and Young's modulus of the films, with a significant influence of the deposition temperature. These mechanical behaviours were finally correlated with the phase occurrence. The f.c.c. phase produced in titanium oxynitride thin films favoured high nanohardness and Young's modulus whereas an amorphous structure largely reduced their mechanical behaviours.

Acknowledgements The authors gratefully acknowledge the financial support of the European Union through the NMP3-CT-2003-505948 project "HARDECOAT". They also thank the Region of Franche-Comté, France.

References

- Scopel WL, Fantini MCA, Alayo MI, Pereyra I (2002) *Thin Sol Films* 413:59
- Richthofen AV, Domnick R, Cremer R, Neuschütz D (1998) *Thin Sol Films* 317:282
- Futsuhara M, Yoshioka K, Takai O (1998) *Thin Sol Films* 317:322
- Martin N, Banakh O, Santo AME, Springer S, Sanjinès R, Takadom J, Lévy F (2001) *Appl Surf Sci* 185:123
- Suzuki M, Saito Y (2001) *Appl Surf Sci* 173:171
- Jung MJ, Nam KH, Chung YM, Boo JH, Han JG (2003) *Surf Coat Technol* 171:71
- Fabreguette F, Imhoff L, Maglione M, Domenichini B, Lucas MCMD, Sibillot P, Bourgeois S, Sacilotti M (2000) *Chem Vap Deposition* 6:1
- Vaz F, Cerqueira P, Rebouta L, Nascimento SMC, Alves E, Goudeau P, Rivière JP, Pischow K, Rijk LD (2004) *Thin Sol Films* 447–448:449
- Kazemeini MH, Berezin AA, Fukuhara N (2000) *Thin Sol Films* 372:70
- Chappé JM, Martin N, Terwagne G, Lintymer J, Gavaille J, Takadom J (2003) *Thin Sol Films* 440:66
- Vaz F, Cerqueira P, Rebouta L, Nascimento SMC, Alves E, Goudeau P, Rivière JP (2003) *Surf Coat Technol* 174–175:197
- Martin N, Sanjinès R, Takadom J, Lévy F (2001) *Surf Coat Technol* 142–144:615
- Nishimura E, Ando M, Onisawa KI, Takabatake M, Minemura T (1996) *Jpn J Appl Phys* 35:2788
- Bally AR, Hones P, Sanjinès R, Schmid PE, Lévy F (2002) *Surf Coat Technol* 108–109:272
- Banakh O, Schmid PE, Sanjinès R, Lévy F (2002) *Surf Coat Technol* 151–152:272

16. Chappé JM, Martin N, Pierson JF, Terwagne G, Lintymer J, Gavaille J, Takadom J (2004) *Appl Surf Sci* 225:29
17. Shigesato Y, Hayashi Y, Masui A, Haranou T (1991) *Jpn J Appl Phys* 30:814
18. Nakada T, Ohkubo Y, Kuniok A (1996) *Jpn J Appl Phys* 30:3344
19. Onisawa KI, Nishimura E, Ando M, Satou T, Takabatake M, Minemura T (1997) *MRS 1996 Spring Meeting, MRS Symposium Proceeding* 424:341
20. Lobl P, Huppertz M, Mergel D (1994) *Thin Sol Films* 251:72
21. Hones P, Diserens M, Lévy F (1999) *Surf Coat Technol* 120–121:277
22. Oliver WC, Pharr GM (1992) *J Mater Res* 7:1564
23. Jönsson B, Hogmark S (1984) *Thin Sol Films* 377–378:257
24. Makino Y, Nose M, Tanaka T, Misawa M, Tanimoto A, Nakai T, Kato K, Nogi K (1998) *Surf Coat Technol* 98:934
25. Veprek S, Reiprich S, Shizhi L (1995) *Appl Phys Lett* 66:2640
26. Diserens M, Patscheider J, Lévy F (1999) *Surf Coat Technol* 120–121:158